

Voronoi cells, fractal dimensions and fibre composites

J. SUMMERSCALES,* F. J. GUILD,† N. R. L. PEARCE‡ & P. M. RUSSELL§

**Department of Mechanical and Marine Engineering, University of Plymouth, Drake Circus, Plymouth PL4 8AA, U.K.*

†*Department of Mechanical Engineering, University of Bristol, U.K.*

‡*Devonport Management Limited, Plymouth, U.K.*

§*Department of Biological Sciences, University of Plymouth, U.K.*

Key words. Composites, fractal dimensions, tessellation, Voronoi cells.

Summary

The use of fibre-reinforced polymer matrix composite materials is growing at a faster rate than the gross domestic product (GDP) in many countries. An improved understanding of their processing and mechanical behaviour would extend the potential applications of these materials. For unidirectional composites, it is predicted that localized absence of fibres is related to longitudinal compression failure. The use of woven reinforcements permits more effective manufacture than for unidirectional fibres. It has been demonstrated experimentally that compression strengths of woven composites are reduced when fibres are clustered. Summerscales predicted that clustering of fibres would increase the permeability of the reinforcement and hence expedite the processing of these materials. Commercial fabrics are available which employ this concept using flow-enhancing bound tows. The net effect of clustering fibres is to enhance processability whilst reducing the mechanical properties.

The effects reported above were qualitative correlations. To improve the design tools for reinforcement fabrics we have sought to quantify the changes in the micro/meso-structure of woven reinforcement fabrics. Gross differences in the appearance of laminate sections are apparent for different weave styles. The use of automated image analysis is essential for the quantification of subtle changes in fabric architecture. This paper considers Voronoi tessellation and fractal dimensions for the quantification of the microstructures of woven fibre-reinforced composites. It reviews our studies in the last decade of the process-property-structure relationships for commercial and experimental fabric reinforcements in an attempt to resolve the processing vs. properties dilemma. A new flow-enhancement concept has been developed which has a reduced impact on laminate mechanical properties.

Introduction

The manufacture of fibre reinforced composites has been reviewed by Åström (1997), Gutowski (1997) and Davé & Loos (1999). Resin transfer moulding (RTM) (van Harten, 1993; Potter, 1997; Rudd *et al.*, 1997; Kruckenberg & Paton, 1998; Benjamin & Beckwith, 1999) is emerging as the most probable route to mass production for composite components of complex shape. In RTM a mould is loaded with dry fibres, resin then flows into the dry fabric stack and the resin cures to produce a solid component. The success of the process is critically dependent on the rate at which the resin percolates through the fibres. The Darcy (1856) equation is commonly used for simulation of the process. For a fixed geometry, the flow rate is proportional to the pressure gradient and inversely proportional to the resin viscosity. The constant of proportionality is known as the permeability of the porous medium. Summerscales (1993b) predicted that clustering of fibres would increase the resin flow rate in the reinforcement and hence expedite the processing of these materials. Thirion *et al.* (1988) have reported commercial fabrics which employ this concept using flow-enhancing bound tows.

Unidirectional (UD) fibres offer the highest mechanical performance when stresses are primarily in either tension or compression along the fibre axis. For more uniformly distributed stresses, it is common to use cross/angle-ply UD fibre composites. However, the absence of transverse reinforcement within each layer makes these materials liable to splitting parallel to the fibres. For applications where high stiffness and high strength are required together with toughness, woven composites can provide a reasonable balance of stiffness, strength and toughness whilst offering improved processability.

For unidirectional composites, the finite element method (FEM) has been used to predict that the type of packing (Wisnom, 1990) or the degree of randomness (Guild *et al.*, 1990) affects the transverse modulus. Furthermore, FEM

has indicated that localized absence of fibres is related to longitudinal compression failure (Guild *et al.*, 1989). Basford *et al.* (1995) have demonstrated experimentally that compression strengths of woven composites were reduced when fibres were more clustered. The net effect of clustering fibres is generally to enhance processability whilst reducing the mechanical properties.

The effects reported above were qualitative correlations. To improve the design tools for reinforcement fabrics we have sought to quantify the changes in the micro/meso-structure of woven reinforcement fabrics. Gross differences in the appearance of materialographic sections are apparent for different weave styles. For subtle variations within a single weave style, the eye cannot easily discern changes. The use of automated image analysis (Guild & Summerscales, 1993, Summerscales, 1998) is essential for the quantification of subtle changes in fabric architecture.

The microstructure of fibre reinforced composites is normally defined by specifying the form of the reinforcement and quantified by measuring the fibre volume fraction and the fibre length/orientation distributions. These data may be insufficient where clustering of fibres occurs. The classification of structured populations can be achieved by a variety of parameters. Early techniques included nearest-neighbour analysis (Clark & Evans, 1954), chi-squared analysis for point patterns (Davis, 1974), quadrat analysis (Greig-Smith, 1952), mean free path and mean random spacing (Cribb, 1978), space auto-correlograms (Mirza, 1970), area fraction variance analysis and mean intercept length analysis (Li *et al.*, 1992) and (for hybrid composites) contiguity index (Short & Summerscales, 1984). More recently the classification of the structures within composite materials has used either tessellation techniques (Summerscales *et al.*, 1993a; Pyrz, 1994, 2000a, b; Ghosh *et al.*, 1997) or fractal dimensions (Taya *et al.*, 1991; Cross, 1994; Worrall & Wells, 1996).

This paper will consider Voronoi tessellation and fractal dimensions for quantification of the microstructures of woven fibre-reinforced composites and will review the process-property-structure relationships for commercial and experimental fabric reinforcement materials studied experimentally in an attempt to resolve the processing vs. properties dilemma.

Experimental

Materials

Three sets of woven carbon fibre reinforcement fabrics were studied in the following temporal sequence:

- Carr Reinforcements twill fabric with bound flow-enhancing tows (FET)
- Brochier twill, satin and Injectex FET satin
- Carr Reinforcements twill fabric with new concept FET

Carr fabrics with bound FET. The Carr fabrics with bound FET were based on a 380 g m^{-2} 6K carbon 2×2 twill fabric (Fig. 1). The flow enhancement was achieved by binding regularly spaced weft tows to constrain these tows to remain approximately elliptical under compression, thereby creating large pore spaces adjacent to the FET. There were four variants plus the reference base fabric:

- fabric twill = normal
- fabric 156 = 12.5% FET (1 in 8)
- fabric 150 = 17% FET (1 in 6)
- fabric 148 = 25% FET (1 in 4)
- fabric 126 = 50% FET (1 in 2)

The permeating fluids were Scott Bader Resin E (initial ambient viscosity (IAV): 4600 mPa s [$1 \text{ mPa s} = 1 \text{ centipoise}$]) and Jotun 4210 (IAV = 2600 mPa s) unsaturated polyester resins. The results have been reported more fully elsewhere (Griffin *et al.*, 1995a, b; Summerscales *et al.*, 1995; Guild *et al.*, 1996).

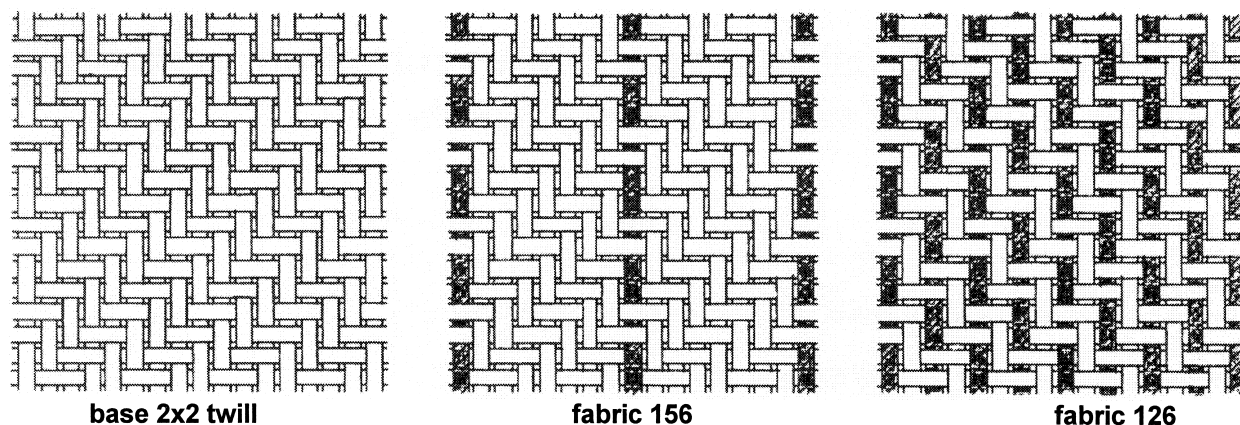


Fig. 1. Schematics of Carr fabrics

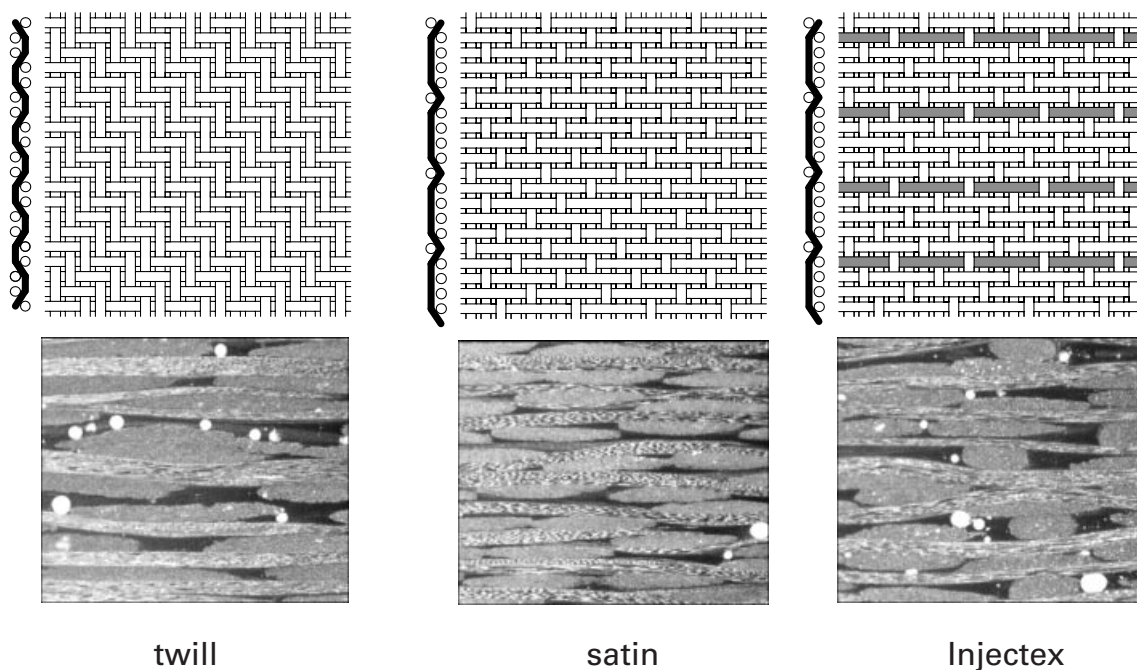


Fig. 2. Schematics and transverse micrographs of Brochier weaves. Image frame is 3.6×3.0 mm.

Brochier fabrics. The Brochier fabrics were all 290 g m^{-2} 6K carbon fibre fabrics (Fig. 2):

- 2×2 twill (designated E3853/G986)
- normal 5-harness satin (designated E3833/G963)
- flow-enhanced Injectex 5-harness satin (every fifth tow bound in one direction, designated E3795)

The permeating fluid was Ciba-Geigy LY564-1/HY2954 epoxy resin (IAV ~ 600 mPa s). The results have been reported more fully elsewhere (Pearce *et al.*, 1998a, b).

New concept Carr fabrics. The new concept Carr fabrics are based on a 372 g m^{-2} 6K carbon 2×2 twill fabric. Flow enhancement is achieved by substitution of some 6K weft tows by 3K tows with a consequent reduction in fabric areal weight (see Table 1).

It is not possible to discern differences between these fabrics with the unaided eye either for dry fabric or sectioned composites. The permeating fluid was SP Ampreg

26 epoxy resin with slow hardener (IAV = 310 mPa s). The results have been reported more fully elsewhere (Pearce *et al.*, 2000).

Measurement of permeability/fabrication of test plates. The composite plates were manufactured during radial flow permeability experiments conducted in a glass-topped aluminium mould with controlled cavity depth. The apparatus and technique, as used for the Brochier fabrics, has been described elsewhere (Carter *et al.*, 1996) and is subject to progressive refinement. Figure 3 shows frame-grabbed images of the advancing flow front during a typical determination of permeability. The images were taken at 36, 201 and 653 s into mould fill. Carter *et al.* (1995) have published the theory used for calculation of the permeability.

Microscopical analysis

Preparation. The woven fabric composites were sampled in both warp and weft directions. Individual pieces of full specimen thickness by up to 25 mm length were mounted by casting in cylindrical pots. Each block was polished in six stages to $1 \mu\text{m}$ and finished with AlSiO_2 for 2 min (Pearce *et al.*, 1998a, b, 2000).

Image analysis. Image analysis was undertaken using a Quantimet 570 image analysis system. The following features were measured: individual void areas, numbers of voids, total void area, counts and areas of pore space.

Table 1. New concept Carr fabrics.

Fabric	Description	Areal weight (g m^{-2})
D	normal twill	372
C	14% FET (1 in 6)	358
B	20% FET (1 in 4)	353
A	33% FET (1 in 2)	340

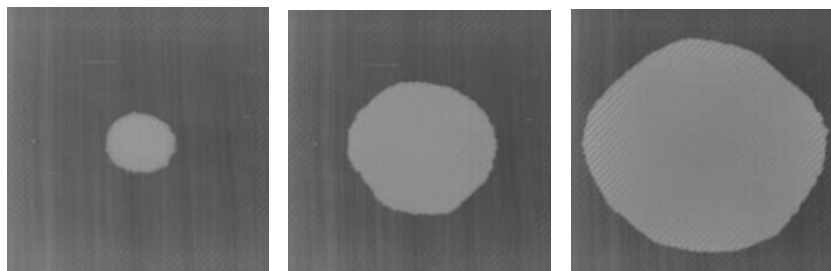


Fig. 3. Frame-grabbed images of a typical radial flow permeability experiment at 36, 201 and 653 s. The square mould has an edge length of 440 mm.

Dirichlet tessellations are constructed such that any point within a cell is closer to the centre of gravity of the feature within that cell than the centre of gravity of any other cell. The boundaries between Dirichlet cells are straight lines, which are in effect the perpendicular bisectors between the centres of gravity of features. Dirichlet tessellation characterizes clustering from the positions of the features.

We have used a specific form of tessellation, known as the Voronoi cell, to characterize the clustering of the features. The features are 'grown' until the surfaces meet and fill the whole space. This normally results in non-linear boundaries between cells. Characterization of clustering by growing techniques is strongly influenced by the size and shape of the features as well as their positions. A rigorous treatment of the spatial statistics is given in Cressie (1993). Figure 4(a) illustrates how, for individual filaments within a bundle, each point in space is assigned to the nearest particle and Fig. 4(b) shows the boundaries constructed from this information. The cells of the tessellation are then analysed to characterize the regions influenced by the non-overlapping particles. The parameters recorded were area, maximum width (horizontal feret), maximum height (vertical feret), perimeter and x - and y -centres of gravity.

To determine the fractal dimension, the microscope image is recorded with 256 grey levels. For example, in Fig. 5 we

use a double threshold. Surface breaking voids are filled with talc and appear white to permit them to be quantified separately. They are then converted to black along with all the other (darker) intertow pore space by careful selection of threshold levels. The tows are then represented by white. The whole image is mapped with a grid of boxes and those boxes containing any pore space are flagged (Fig. 5). A range of square box sizes is used. In each case, the pore space area is measured as the total 'flagged' area. The log (area of filled boxes) is plotted against log (box size). This is known as a Richardson plot. The slope of the graph is the fractal dimension (δ) and gives a unique measurement of the pore space size and distribution. The raw value returned by this process is reported here (note that this value is 0 for a line and 1 for an area. For more conventional representations of dimensions it is necessary to increase this number by unity). The measurement details are summarized in Table 2.

Mechanical testing. Mechanical testing was conducted using CRAG test methods (Curtis, 1988):

- Tensile properties were measured using CRAG method 302 at 5 mm min^{-1} crosshead displacement in an Instron 1175 screw-driven universal testing machine with a 100 kN load cell.

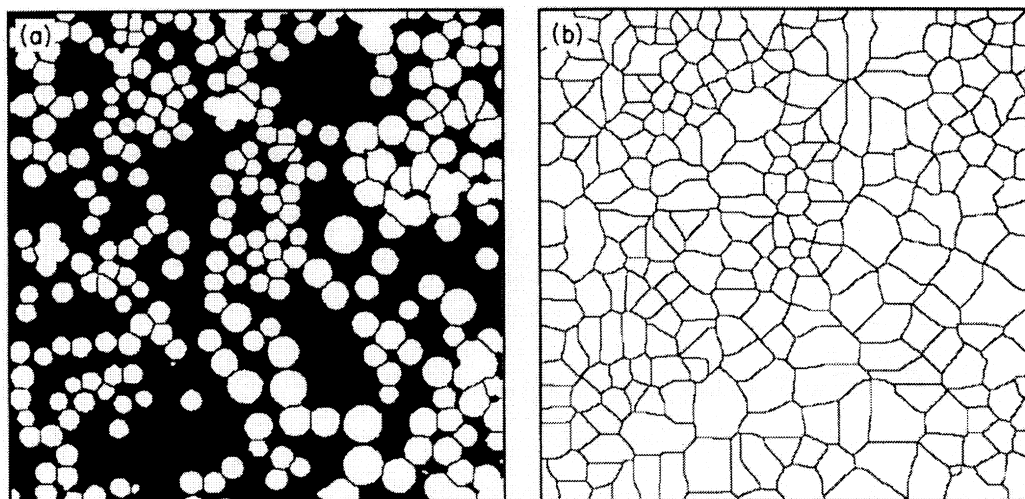


Fig. 4. Voronoi tessellation of a section of glass fibre composite (fibre diameters $\sim 10\text{--}30 \text{ mm}$).

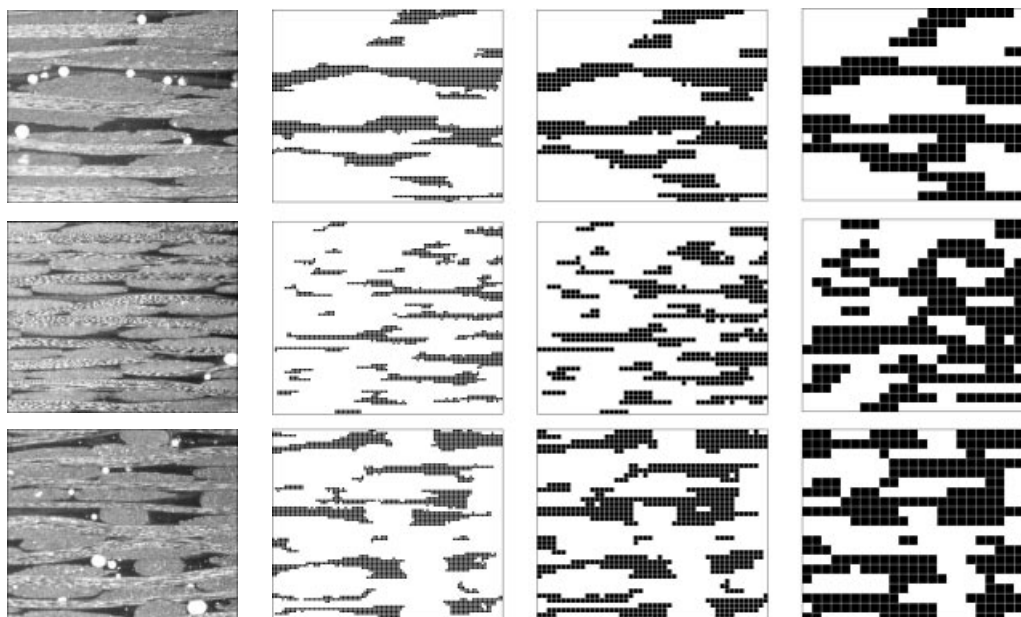


Fig. 5. Sections of Brochier weaves with sample frames from the determination of fractal dimensions. Top row: twill, middle row: satin, bottom row: Injectex. Image frame is 3.6×3.0 mm. Column 1: 480×400 pixel grey image, column 2: 4×4 pixel boxes, column 3: 9×9 pixel boxes, column 4: 19×19 pixel boxes.

- Compression properties were measured using CRAG method 401 at an actuator displacement speed of 2.4 mm min^{-1} in an Instron 8500 servo-hydraulic universal testing machine with a 200 kN load cell.

except where otherwise stated (i.e. Carr bound FET). All specimens were monitored with TMG 350 Ω 12.5 mm strain gauges fed to a Strawberry Tree data logger recording at 10 Hz. Secant moduli were calculated at $2500 \mu\epsilon$.

Results

Carr bound tow FET fabrics

Initial attempts to quantify the microstructure of woven fabrics were conducted on Carr fabrics with bound FET. The

areas of pore space were collected and histograms were drawn: for example, fabric 126 data are shown in Fig. 6(a). Comparing the histograms, it was apparent that different shapes of histograms were associated with the different fabrics. The differences in the data are clearest when the cumulative curves are plotted as the number of zones less than a given size. These cumulative curves, for all five fabrics, are shown in Fig. 6(b). The cumulative number has been 'normalised' to account for the small differences in total area measured for the different fabrics. This plot is truncated at small pore space areas corresponding to $\sim 2\%$ of the area of a typical tow. The relative separation of the plots at around 0.05 mm^2 appears to correlate with the relative values of permeability (Fig. 7), although the range of flow areas chosen is somewhat arbitrary.

Table 2. Details of image analysis for determination of fractal dimensions.

	Brochier	Brochier	Carr new concept
Published reference	Pearce <i>et al.</i> , 1998a	Pearce <i>et al.</i> , 1998b	Pearce <i>et al.</i> 2000
Pixel frame	512×400	480×400	480×480
Analysis frame area (mm)	4×3.125	3.6×3.0	2.2×2.2
Linear resolution (nm/pixel)	7812	7500	4583
Contiguous frames per sample	6	3	4
Measured area (mm)	24×3.125	10.8×3	8.8×2.2
Specimens per fabric	1	10	3
Total area per fabric ($\text{mm}^2/\text{fabric}$)	75	324	58

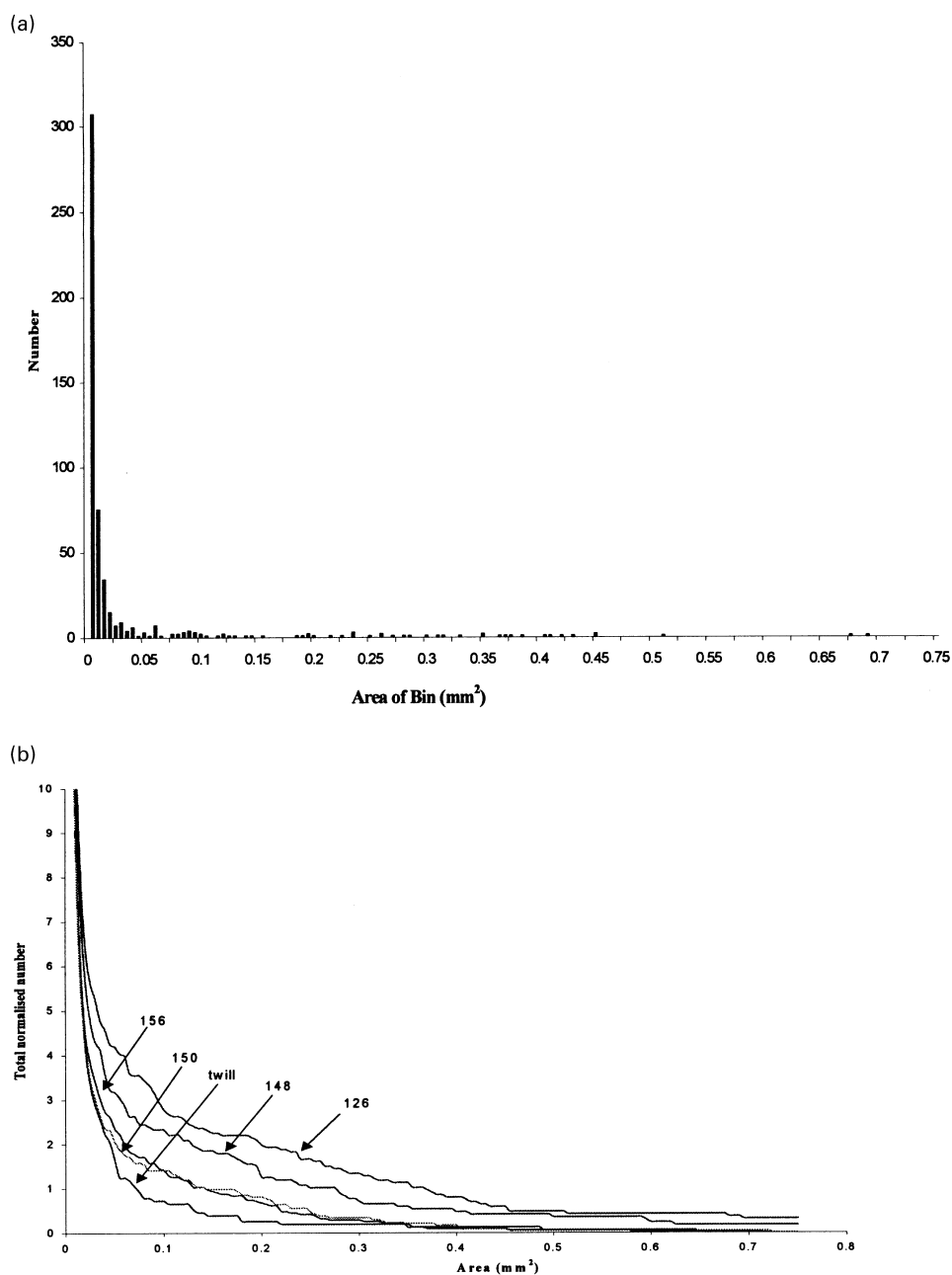


Fig. 6. (a) Histogram of pore space areas for Carr fabric 126. (b) Cumulative curve of pore space zones less than a given value for Carr fabrics.

Basford *et al.* (1995) measured mechanical properties for these composites at constant fibre volume fraction in the Instron 1175 screw-driven test machine. Both the compression strengths (CRAG method 401 at 2 mm min^{-1}) and the apparent interlaminar shear strengths (CRAG method 100 at 1 mm min^{-1}) decreased with increasing proportion of flow-enhancing tows at constant fibre volume fraction ($\sim 43\%$). The mean values for six specimens of each type are shown in Fig. 8. The maximum standard deviation was 26 MPa for compression strengths and 5.2 MPa for ILSS.

Brochier fabrics

The use of fractal dimensions to analyse the pore space features normal to the flow enhancing tows clearly differentiates between the structures of the Brochier fabrics: Injectex FET ($\delta = 0.356$), twill ($\delta = 0.364$) and satin without FET ($\delta = 0.424$). The weave style influences pore space distribution (and hence permeability) and fibre crimp (and hence mechanical properties). The relative permeabilities of the fabrics are shown in Fig. 9 and the

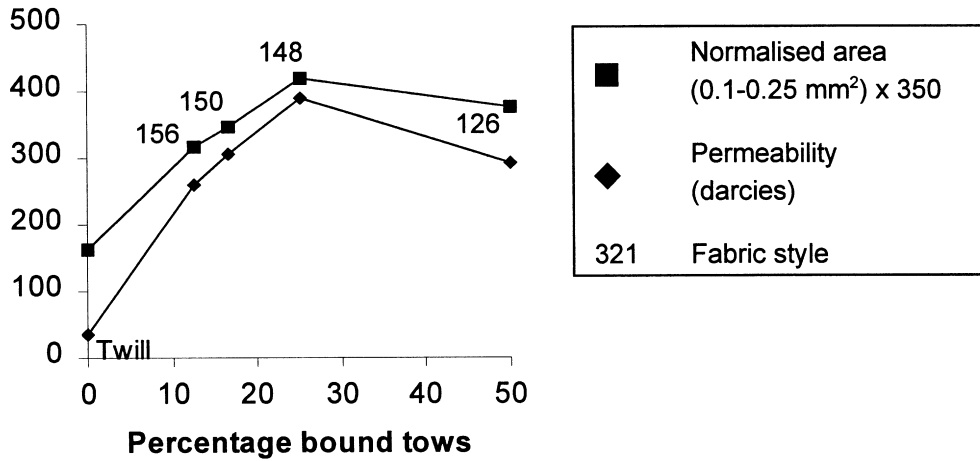


Fig. 7. Flow area and permeability plotted against percentage FET for Carr bound tow FET.

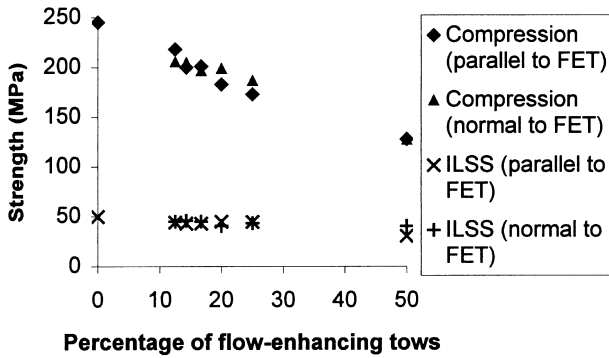


Fig. 8. Strengths of Carr fabrics plotted against proportion of flow-enhancing tows in the weft.

Table 3. Mechanical properties of Brochier fabrics normal to the FET.

	Compression	Tension
Young's moduli (GPa)		
Injectex	50 ± 1.0	52 ± 2.4
Satin	54 ± 1.1	57 ± 1.3
Twill	51 ± 1.3	54 ± 1.3
Strengths (MPa)		
Injectex	339 ± 37.2	767 ± 42.7
Satin	458 ± 66.2	906 ± 34.3
Twill	360 ± 56.5	781 ± 46.2

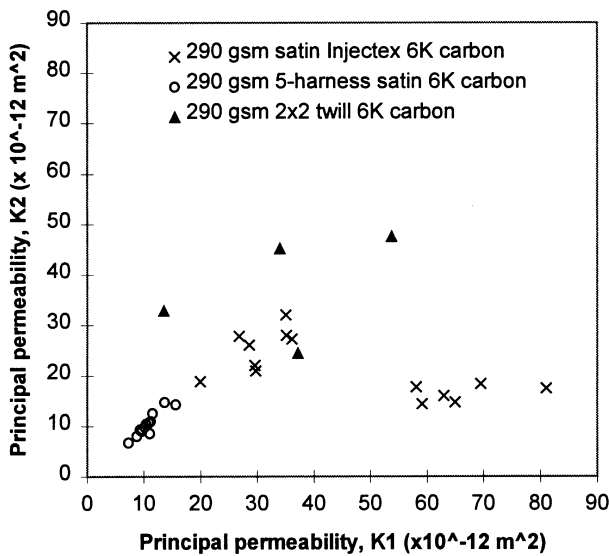


Fig. 9. Principal in-plane permeabilities in x (K1) and y (K2) of the Brochier fabrics (units of permeability are $\times 10^{-12} \text{ m}^2$).

mechanical properties are presented in Table 3. The ranked experimental results (Table 4) for the Brochier fabrics clearly show that a conflict exists between processing (satin is the worst fabric) and mechanical properties (satin is the best fabric).

Table 4. Ranking of measured properties and quantified microstructures normal to the FET.

	Lowest	Middle	Highest
Processing			
Permeability	Satin	Injectex	Twill
Mechanical properties			
Tensile Strength/Moduli	Injectex	Twill	Satin
Compressive Strength/Moduli	Injectex	Twill	Satin
Fractal analysis			
Inter-tow pore space area	Satin	Twill	Injectex
Fractal dimension (δ)	Injectex	Twill	Satin

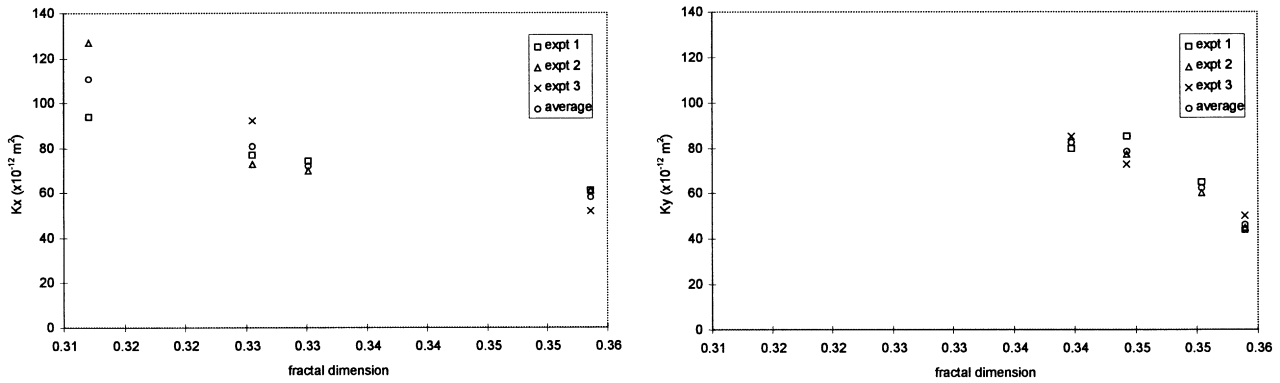


Fig. 10. Permeability plotted against fractal dimension for weft (left) and warp (right) new concept Carr fabrics.

New concept Carr fabrics

For the new concept Carr fabrics, the permeabilities and fractal dimensions are both ranked in the sequence ACBD (Fig. 10). The fractal dimension (δ) of the base fabric (D) is essentially the same in warp and weft. The value of δ is similar for the warp direction for all fabrics.

The mechanical properties of the new concept Carr fabrics are very similar and show very low scatter for all directions without FET: both warp and weft in the base fabric and the warp direction in FET fabrics (Table 5). The higher scatter in the tensile strength is attributed to the alignment of the mechanical grips in the screw-driven

Table 5. Mechanical properties of new concept Carr fabrics.

Secant moduli (GPa \pm % SD)				
	Compression		Tension	
	Warp	Weft	Warp	Weft
A	47 \pm 1.10	40 \pm 0.75	49 \pm 0.89	42 \pm 0.37
B	48 \pm 1.02	43 \pm 0.58	49 \pm 1.34	45 \pm 0.82
C	47 \pm 1.24	44 \pm 0.38	49 \pm 0.70	45 \pm 1.25
D	48 \pm 0.51	47 \pm 0.44	50 \pm 0.38	49 \pm 0.84
%SD	0.58	5.28	0.58	5.70
Strength (MPa \pm % SD)				
	Compression		Tension	
	Warp	Weft	Warp	Weft
A	315 \pm 1.01	317 \pm 0.25	706 \pm 4.49	542 \pm 3.41
B	317 \pm 0.14	316 \pm 0.86	704 \pm 2.88	595 \pm 3.51
C	317 \pm 0.23	314 \pm 1.55	718 \pm 4.08	556 \pm 4.97
D	317 \pm 0.22	317 \pm 0.18	720 \pm 4.93	602 \pm 3.44
%SD	0.24	0.33	1.01	4.43

machine being less accurate than that of the hydraulic grips in the servo-hydraulic machine.

The weft compression and weft tension moduli decrease broadly in line with the expectations from rule-of-mixtures. The weft tension strength decreases in the same sequence as the fractal dimension (Fig. 11). The compression and warp tension strengths are barely affected by the presence of the FET.

Comparison of different fabric sets

Table 6 and Fig. 12 present the fractal dimensions and measured permeabilities of the Brochier and new concept Carr FET fabrics. The point at the right-hand end of the twill fabric line is for Brochier material of a lower areal weight, whereas the other points are for new concept Carr fabrics. Note that both the Brochier satin and the new concept Carr fabrics can have permeability doubled by the insertion of flow-enhancement tows.

Conclusion

In this paper we have considered routes to permit the microstructural features of woven composites to be quantified. These techniques have been applied to real woven

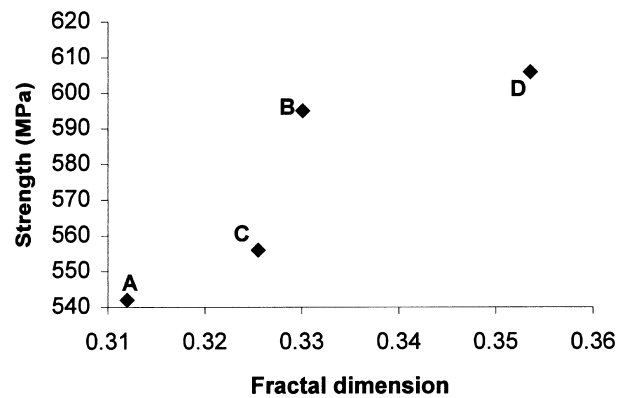
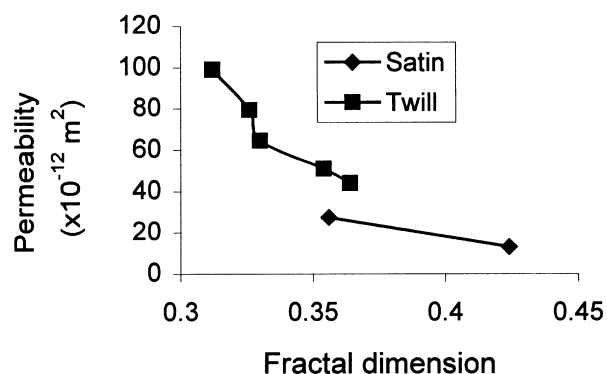


Fig. 11. Weft tensile strength plotted against fractal dimension for new concept Carr fabrics.

Table 6. Fractal dimensions and permeabilities for two sets of fabric.

Fabric	Fractal dimensions	Permeability (10^{-12} m^2)
Brochier fabrics: 290 g m^{-2}		
Satin (no FET)	0.424	8–18
Twill	0.364	34–54
Injectex FET	0.356	19–36
Carr fabrics: $340\text{--}372 \text{ g m}^{-2}$		
D (base twill)	0.354	41–61
B (20% FET)	0.330	54–75
C (14% FET)	0.326	67–92
A (33% FET)	0.312	72–126

**Fig. 12.** Permeability plotted against fractal dimension for Brochier and new concept Carr fabrics.

reinforcement materials. Certain processing and mechanical properties can be correlated to the quantified microstructures, even when no differences can be discerned by eye. New concept Carr fabrics have been developed which appear to achieve appropriate process-property-structure relationships for commercial application, i.e. flow enhancement with minimal reduction in mechanical properties.

Acknowledgements

The authors wish to express their gratitude to the European Union for BRITE/EurAM II grant BE5477 and to EPSRC for research grants GR/J77405 and GR/K04699 which funded this work. Especial thanks are due to Carr Reinforcements Limited (Stockport, U.K.) for weaving fabrics specifically for this research. Thanks are due to colleagues Eddie Carter, Tony Fell, Patrick Griffin, Eirian Jones, Rana Moyeed and Tim Searle for their helpful discussions and/or assistance with the experimental work. We are also grateful to the anonymous referees for their respective comments on the manuscript.

References

- Åström, B.T. (1997) *Manufacturing of Polymer Composites*. Chapman & Hall, London.
- Basford, D.M., Griffin, P.R., Grove, S.M. & Summerscales, J. (1995) The relationship between mechanical performance and microstructure in composites with flow-enhancing tows. *Composites*, **26**, 675–679.
- Benjamin, W.P. & Beckwith, S.W. (1999) *Resin Transfer Moulding*, SAMPE Monograph 3, Covina, CA.
- Carter, E., Fell, A.W., Griffin, P.R. & Summerscales, J. (1996) Data validation procedures for the automated determination of the two-dimensional permeability tensor of a fabric reinforcement. *Composites Part A: Appl. Sci. Manufacturing*, **27A**, 255–261.
- Carter, E., Fell, A.W. & Summerscales, J. (1995) A simplified model for the derivation of the permeability tensor of an anisotropic fibre bed. *Composites Manufacturing*, **6**, 228–235.
- Clark, P.J. & Evans, F.C. (1954) Distance to the nearest neighbour as a measure of spatial relationships in population. *Ecology*, **35**, 445–453.
- Cressie, N.A.C. (1993) *Statistics for Spatial Data*. John Wiley, New York.
- Cribb, W.R. (1978) Quantitative metallography of polyphase microstructures. *Scripta Metallurgica*, **12**, 893–898.
- Cross, S.S. (1994) The application of fractal geometric analysis to microscopic images. *Micron*, **25**, 101–113.
- Curtis, P.T. (1988) *CRAG Test Methods for the Measurement of the Engineering Properties of Fibre Reinforced Plastics*. Royal Aerospace Establishment Techn Report RAE TR 88 012.
- Darcy, H.P.G. (1856) *Les Fontaines Publiques de la Ville de Dijon*. Dalmont, Paris.
- Davé, R.S. & Loos, A.C. (1999) *Processing of Composites*. Hanser Publishing, Munich.
- Davis, P. (1974) Data description and presentation. *Describing Point Patterns*. Oxford University Press, Oxford, pp. 29–35.
- Ghosh, S., Nowak, Z. & Lee, K. (1997) Tessellation-based computational methods for the characterization and analysis of heterogeneous microstructures. *Composites Sci. Technology*, **57**, 1187–1210.
- Greig-Smith, P. (1952) The use of random and contiguous quadrats in the study of plant communities. *Annals of Botany – London*, **NS16**, 293–316.
- Griffin, P.R., Grove, S.M., Guild, F.J., Russell, P.M. & Summerscales, J. (1995a) The effect of microstructure on flow promotion in resin transfer moulding reinforcement fabrics. *J. Microsc.* **177**, 207–217.
- Griffin, P.R., Grove, S.M., Russell, P.M., Short, D., Summerscales, J., Guild, F.J. & Taylor, E. (1995b) The effect of reinforcement architecture on the long-range flow in fibrous reinforcements. *Comp. Man.*, **6**, 221–228.
- Guild, F.J., Davy, P.J. & Hogg, P.J. (1989) A model for unidirectional composites in longitudinal tension and compression. *Comp. Sci. Techn.* **36**, 7–26.
- Guild, F.J., Davy, P.J. & Hogg, P.J. (1990) A predictive model for the mechanical behaviour of transverse fibre composites. *4th International Conference on Fibre-Reinforced Composites, Liverpool*, 89–99.
- Guild, F.J., Pearce, N.R.L., Griffin, P.R. & Summerscales, J. (1996) Optimisation of reinforcement fabrics for the resin transfer

- moulding of high fibre volume fraction composites. *7th European Conference on Composite Materials, London*, **1**, 273–278.
- Guild, F.J. & Summerscales, J. (1993) Microstructural image analysis applied to fibre composite materials – a review. *Composites*, **24**, 383–394.
- Gutowski, T.G. (1997) *Advanced Composites Manufacturing*. John Wiley, New York.
- van Harten, K. (1993) Production by resin transfer moulding. *Composite Materials in Maritime Structures* (ed. by R. A Shenoi and J F Wellicome), pp. 86–126. Cambridge University Press, Cambridge.
- Kruckenberg, T.M. & Paton, R. (eds) (1998) *Resin Transfer Moulding for Aerospace Structures*. Kluwer Academic Publishers, Dordrecht NL.
- Li, Q.F., Smith, R. & McCartney, D.G. (1992) Quantitative evaluation of fiber distributions in a continuously reinforced aluminium alloy using automatic image analysis. *Materials Characterization*, **28**, 189–203.
- Mirza, K.S.M.A. (1970) A statistical study of the structure of mixtures of particulate solids. PhD Thesis, University of Exeter.
- Pearce, N.R.L., Summerscales, J. & Guild, F.J. (1998a) An investigation into the effects of fibre architecture on the processing and properties of fibre reinforced composites produced by resin transfer moulding. *Composites Part A: Appl. Sci. Manufacturing*, **29A**, 19–27, 707.
- Pearce, N.R.L., Summerscales, J. & Guild, F.J. (1998b) The use of automated image analysis for the investigation of fibre architecture on the processing and properties of fibre reinforced composites made by RTM. *Composites Part A: Appl. Sci. Manufacturing*, **29A**, 829–837.
- Pearce, N.R.L., Summerscales, J. & Guild, F.J. (2000) Improving the resin transfer moulding process for fabric-reinforced composites by modification of the fibre architecture. *Composites Part A: Appl. Sci. Manufacturing*, **31A**, 1433–1441.
- Potter, K. (1997) *Resin Transfer Moulding*. Chapman & Hall, London.
- Pyrz, R. (1994) Quantitative description of the microstructure of composites, Part 1: morphology of unidirectional composite systems. *Comp. Sci. Technology*, **50**, 197–208.
- Pyrz, R. (2000a) Morphological characterization of microstructures. *Comprehensive Composite Materials*, Vol. 1: *Fiber Reinforcements and General Theory of Composites*. Elsevier, Oxford, pp. 465–478.
- Pyrz, R. (2000b) The application of morphological methods to polymer matrix composites. *Comprehensive Composite Materials*, Vol. 2: *Polymer Matrix Composites*. Elsevier, Oxford, pp. 553–576.
- Rudd, C.D., Long, A.C., Kendall, K.N. & Mangin, C.G.E. (1997) *Liquid Composite Moulding*. Woodhead Publishing, Cambridge.
- Short, D. & Summerscales, J. (1984) The definition of microstructures in hybrid reinforced plastics. *5th European Conference of the Society for the Advancement of Materials and Process Engineering, Montreux*. SAMPE, Montreux.
- Summerscales, J. (1993b) A model for the effect of fibre clustering on the flow rate in resin transfer moulding. *Comp. Manu.* **4**, 27–31.
- Summerscales, J. (ed.) (1998) *Microstructural Characterisation of Fibre-Reinforced Composites*, Woodhead, Cambridge.
- Summerscales, J., Griffin, P.R., Grove, S.M. & Guild, F.J. (1995) Quantitative microstructural examination of RTM fabrics designed for enhanced flow. *Comp. Struct.* **32**, 519–529.
- Summerscales, J., Green, D. & Guild, F.J. (1993a) Effect of processing dwell time on the microstructure of a fibre reinforced composite. *J. Microsc.* **169**, 173–182.
- Taya, M., Muramatsu, K., Lloyd, D.J. & Watanabe, R. (1991) Determination of distribution patterns of fillers in composites by micromorphological parameters. *JSME Int J. Series I*, **34**, 198–206.
- Thirion, J.-M., Girardy, H. & Waldvogel, U. (1988) New developments in resin transfer moulding of high-performance composite parts. *Institute of Metals Materials Information Translation of Composites (Paris)*, **28**, 81–84.
- Wisnom, M.R. (1990) Factors affecting the transverse tensile strength of unidirectional continuous silicon carbide fibre reinforced 6061 aluminium. *J. Comp. Mater.* **24**, 707–726.
- Worrall, C.M. & Wells, G.M. (1996) Fibre distribution in discontinuous fibre reinforced plastic: characterisation and effect on material performance. *7th European Conference on Composite Materials, London*, **1**, 247–252.